

Gamma Ray Bursts: Complementarity to Other Cosmological Probes

Meng Su¹, Hong Li^{1,2}, Zuhui Fan¹, and Bo Liu³

1 Department of Astronomy, School of Physics, Peking University, Beijing, 100871, P. R. China

2 Institute of High Energy Physics, Chinese Academy of Sciences, P.O. Box 918-4, Beijing, 100049, P. R. China

3 National Laboratory for Information Science and Technology, Tsinghua University, Beijing, 100084, P. R. China

ABSTRACT

We combine recent long Gamma Ray Bursts (GRBs) sample including 52 objects out to $z=6.3$ compiled from Swift Gamma Ray Bursts by Schaefer (2006) with Type Ia Supernova (SNIa), Cosmic Microwave Background (CMB) and Baryon Oscillation (BAO) to constrain cosmologies. We study the constraints arising from GRBs alone and the complementarity of GRBs to other cosmological probes. To analyze the cosmological role of GRBs, we adopt the Hubble constant as a free parameter with a prior in the range of $H_0 = 72 \pm 8 \text{ km s}^{-1} \text{ Mpc}^{-1}$ instead of a fixed H_0 used in previous studies. By jointly using SNIa gold/SNLS samples and GRBs, the constraints on Ω_M - Ω_Λ parameter space are dramatically improved in comparing with those from SNIa data alone. The complementarity of GRBs is mostly from the sub-sample with $z>1.5$ due to the different parameter degeneracies involved in luminosity distances at different redshifts. Including GRB data in addition to SNIa, BAO and CMB in our analysis, we find that the concordance model with $\Omega_M \sim 0.3$ and $\Omega_\Lambda \sim 0.7$ is still well within 1σ confidence range.

Subject headings: Gamma Rays: bursts — Cosmology: observations, dark energy

¹sxsumeng@pku.edu.cn

1. Introduction

As the three famous observational supports for the Big Bang Cosmology, there are three cosmological "pillars" to support the picture of the accelerating universe: Observations of Type Ia Supernova (SNIa), Cosmic Microwave Background (CMB) and Large Scale Structures of the universe (LSS). According to the combined analysis with all the available observational data, a concordance cosmological model has been obtained (Riess et al. 2004; Astier et al. 2006; Spergel et al. 2006; Tegmark et al. 2006). In the context of Einstein's general relativity, a special sort of building blocks of our universe, named *dark energy*, needs to be introduced (Weinberg 1989; Peebles & Ratra 2003; Copeland et al. 2006)². It began to dominate our universe recently and probably hold the key for the future evolution of the universe. Understanding the nature of dark energy has become one of the most alluring and challenging tasks with profound implications for both cosmology and theoretical physics.

Due to the fundamental importance of dark energy, it is with great motivation to use different cosmological probes to study the property of dark energy with their own advantages. Comparing constraints from different observations can provide important consistency checks of cosmological models, and find potential systematics of each probe, or possibly get inspiration of new physics behind the bias. On the other hand, because of the different parameter degeneracies involved in different observables, combining proper means can greatly break sorts of degeneracies and shrink the allowed parameter space so that to achieve the goal of precision cosmology.

In particular, it has been known for a long time that standard candles spanning a wide range of redshift can be used to tightly constrain cosmological parameters. Since they carry integrated information between sources and observers, we need standard candles from diverse redshifts to understand tomographically the history of the cosmic expansion and further to distinguish different cosmological models. SNIa has been the most successful distance indicator for cosmological studies. However, it is difficult to observe very high redshift SNIa. On the other hand, long gamma-ray bursts (GRBs) have been known as the most powerful events happened in the universe. After the discovery of the X-ray afterglow of GRB970228 (Costa et al. 1997), the major breakthrough in understanding GRBs, a great effort has been dedicated to find tight relations between observables that could potentially "calibrate" GRBs as independent probes in cosmology (Amati et al. 2002; Ghirlanda et al. 2004a; Liang & Zhang 2005; Firmani et al. 2005; Lamb et al. 2005; Wang & Dai 2006; Firmani et al. 2006a; Firmani et al. 2006b). There are several conspicuous advantages of

²Another possibility is so-called Modified Gravity. See e.g. Lue (2006) for a recent review for DGP model and Song et al. (2006) for the structure formation within this scenario.

GRB to be a unique means for cosmological studies. The huge emitted power of GRBs makes them detectable at $z \sim 20$ or even higher, deep within the range of the epoch of reionization (Schaefer 2003; Ghirlanda et al. 2004b; Dai, et al. 2004, Hooper & Dodelson 2006). They are dust absorption-free tracers of the massive star formation in the universe (Pacsynski 1998; Blain & Natarajan 2000, Lamb & Reichart 2000; Bromm & Loeb 2002; Lloyd-Ronning et al. 2002; Firmani et al. 2004; Friedman & Bloom 2005; Schaefer 2006). However, because of the large dispersion of energies (Bloom et al. 2003) and the difficulties to determine their redshifts (Pelangeon et al. 2006 and references therein), GRBs have not been considered as veracious lighthouse for a long time.

Recently, Ghirlanda et al.(2004a) found that for GRBs the total energy emitted in γ -rays (E_γ), after a proper collimated correction, correlates tightly with the peak spectral energy E_{peak} (in a νF_ν plot). Thus, the isotropically equivalent burst energy could be determined accurately enough to be used practically for cosmological studies. Firmani et al. (2006a) discovered a new correlation among emission properties of GRBs, which involves the isotropic peak luminosity L_{iso} , the peak energy E_{peak} in the spectrum, and the "high signal" time-scale $T_{0.45}$ used to characterize the variability of GRBs. In the source rest-frame, this relation follows as: $L_{\text{iso}} = \tilde{K} E_{\text{peak}}^{1.62} T_{0.45}^{-0.49}$, with \tilde{K} being a constant. GRBs are thus becoming feasible distance indicators. As they are the unique probe of high redshift universe, GRBs might play important roles in dark energy studies, especially if dark energy exhibits interesting behaviors at high redshifts (but also see Linder & Huterer 2003; Aldering et al. 2006).

In this *letter* we study the cosmological constraints by recent GRBs sample including 52 GRBs out to $z=6.3$ (Schaefer 2006). As we mainly demonstrate the cosmological roles of GRBs, we focus on Λ CDM models. There are three relevant parameters H_0 , Ω_m and Ω_Λ . We concentrate on the constraints on $(\Omega_M, \Omega_\Lambda)$. For H_0 , instead of using a fixed value as in previous studies, we treat it as a free parameter with a uniform prior in the range of $H_0 = 72 \pm 8 \text{ km s}^{-1} \text{ Mpc}^{-1}$ to get more realistic constraints from GRBs. We then combine GRBs with SNIa "gold" (Riess et al. 2004)/SNLS (Astier et al. 2006) samples, the information from WMAP three-year results (Spergel et al. 2006), and BAO from SDSS (Eisenstein et al. 2005) to study their joint constraints.

2. Observational Data

We take the advantage of the recent GRB sample compiled by Schaefer (2006) including 52 bursts with properly estimated and corrected redshifts to investigate the cosmological constraints. The redshift of the sample extends to $z=6.3$ with 25 objects having $z > 1.5$. Mosquera Cuesta et al. (2006) showed the distance modulus-redshift relation of this sample

explicitly. Upon using these distance modulus, we fully aware of the circulation problem associated with GRBs as cosmological probes (e.g. Firmani et al. 2006c). As the correlations are calibrated in a cosmologically model-dependent way due to the lack of a suitable set of low redshift GRBs, the consistent analyses of the data should regard the cosmological parameters as free ones in finding quantitative correlation relations, and then study their constraints coherently (Ghirlanda et al. 2006). On the other hand, it has been shown that the correlation parameters (e.g. Firmani et al. 2006c) are not very sensitive to cosmological models although the scatters do. Therefore we do not expect large biases if using a given set of distance modulus calibrated with a fiducial cosmological model to analyze their cosmological constraints. In this paper, we take the distance modulus calculated by Schaefer (2006; Mosquera Cuesta et al. 2006) without any corrections for the circulation problem.

We also use SNIa gold sample and SNLS data in our analyses. The Riess gold sample contains 157 data including 14 high redshift SNIa with $z > 0.9$ (Riess et al. 2004). The SNLS sample consists of 44 nearby ($0.015 < z < 0.125$) objects assembled from the literature, and 73 distant SNIa ($0.15 < z < 1.00$) discovered and carefully followed during the first year of SNLS (Astier et al. 2006). For the cosmological fits, two of the SNLS data points were excluded because they are outliers in the Hubble diagram. To analyze the role of GRB and to study the combined constraints, we further make use of the shift parameter $\mathcal{R} = \sqrt{\Omega_m^0} \int_0^{z_{\text{dec}}} \frac{dz}{E(z)}$, determined from WMAP, CBI and ACBAR (Wang & Mukherjee 2006), and the parameter A measured from SDSS (Eisenstein et al. 2005) that is defined as $A = \sqrt{\Omega_m^0} E(z_1)^{-1/3} \left[\frac{1}{z_1} \int_0^{z_1} \frac{dz}{E(z)} \right]^{2/3}$ with $z_1 = 0.35$. The CMB shift parameter contains the main information for the scale of the first acoustic peak in the TT spectrum, and is the most relevant one for constraining dark energy properties. Recently, the new SDSS LRG data were released (Tegmark et al. 2006), and the corresponding power spectrum was analyzed. The BAO peaks are clearly seen in the power spectrum, which, together with the overall shape, put tight constraints on model parameters.

For the fitting methodology, we use the standard χ^2 minimization method. We also choose standard parametrization of Λ CDM model instead of the non-parametric method (e.g. Daly & Djorgovski 2004). It is known that parameter estimates depend sensitively on the assumed priors on other parameters. In our study, we choose the allowed range of the Hubble constant $H_0 = 72 \pm 8 \text{ km s}^{-1} \text{ Mpc}^{-1}$ resulting from the Hubble Space Telescope Key Project with a uniform prior (Freedman et al. 2001), and marginalize over H_0 to get two-dimensional constraints for Ω_M and Ω_Λ . It is noted that most of the previous work using GRBs to constrain cosmological parameters took a fixed value of H_0 .

3. Complementarity of GRBs to Other Probes

In this section, we study the cosmological constraints using data sets we have discussed above.

Fig.1 shows confidence-level contours for the Λ CDM model using the GRBs sample. We divide the sample into two sub-samples with $z < 1.5$ including 27 objects and $z > 1.5$ including 25 objects, respectively. The dot-dashed lines are the results from the $z > 1.5$ sub-sample with the minimum $\chi^2 = 28.22$ at $\Omega_m = 0.32$ and $\Omega_\Lambda = 0.93$. The dashed lines correspond to the $z < 1.5$ sub-sample with the minimum $\chi^2 = 36.68$ at $\Omega_m = 0.56$ and $\Omega_\Lambda = 1.48$. The solid lines show the constraints resulting from the full GRBs sample with the minimum $\chi^2 = 65.78$ occurring at $\Omega_M = 0.43$, and $\Omega_\Lambda = 0.91$. We note that the degeneracy direction from the $z < 1.5$ sub-sample is similar to that from SNLS SNIa sample, but the contours are much larger due to larger error bars in GRB data. Thus with similar redshift distributions, GRBs cannot provide much additional information in the parameter constraints in comparison with that of SNIa. The constraints from the high-redshift sub-sample have degeneracies rotating toward Ω_Λ . We also show the results from the full GRBs sample with a fixed Hubble constant $H_0 = 74 \text{ km s}^{-1}\text{Mpc}^{-1}$ (short dashed lines). The corresponding minimum χ^2 is $\chi^2 = 65.79$ at $\Omega_m = 0.43$ and $\Omega_\Lambda = 0.91$. The contours are much more narrow than the solid ones. This shows clearly that a strong prior can result an overestimate on the power of a cosmological probe. It is also noted that factitious priors on H_0 can result in strongly biased constraints. For $H_0 = 68 \text{ km s}^{-1}\text{Mpc}^{-1}$, the corresponding minimum is $\chi^2 = 68.08$ at $\Omega_m = 0.53$ and $\Omega_\Lambda = 0.38$. For $H_0 = 80 \text{ km s}^{-1}\text{Mpc}^{-1}$, the corresponding minimum is $\chi^2 = 68.53$ at $\Omega_m = 0.32$ and $\Omega_\Lambda = 1.13$.

In Fig.2, we show the results from combining SNLS SNIa data with the full GRBs sample and with the $z > 1.5$ sub-sample, respectively. The short dashed lines correspond to the constraints from the SNLS sample. The dashed lines and the solid lines correspond to constraints by combining SNLS with the $z > 1.5$ GRB sub-sample (the minimum $\chi^2 = 140.35$ at $\Omega_m = 0.45$ and $\Omega_\Lambda = 1.01$) and with full GRBs sample (the minimum $\chi^2 = 181.62$ at $\Omega_m = 0.46$ and $\Omega_\Lambda = 1.02$), respectively. It is seen clearly that GRBs contribute considerably to the cosmological constraints comparing with that from SNIa alone due to their much more extended redshift range.

In Fig.3, we plot the results of the combined analysis of SNIa + BAO with solid contours and compare it with the constraints from SNIa + full GRB sample (dashed lines). We find that including the information from BAO that tightly constrains the matter content Ω_M , the contribution from GRBs is degraded. On the other hand, the two sets of constraints are largely consistent with each other, indicating the feasibility of using GRBs as cosmological probes. Considering the central values of Ω_M and Ω_Λ , however, there exists some

differences between the results of SNIa+BAO and SNIa+GRBs. These might imply the existence of some unknown systematics for GRBs themselves as cosmological standard candles and/or new phenomena for high-redshift universe. These apparent differences deserve further investigations.

Fig.4 shows the confidence contours of the combined analyses including CMB. The results from BAO alone, and from the CMB shift parameter are shown in dotted and short dashed lines, respectively. The constraints from the combined GRB+CMB+BAO and CMB+BAO+SNIa are plotted, respectively in dot-dashed and dashed lines. The solid lines are the constraints from CMB+BAO+SNIa+GRBs. The constraints from GRB+CMB+BAO are less restrictive than, but consistent with those from CMB+BAO+SNIa. The concordance model is well within the 68.4% confidence level.

4. Discussion and Conclusion

In this *letter*, we study the role of GRBs in constraining cosmological parameters using the recent GRB sample including 52 GRBs out to $z=6.3$ (Schaefer 2006). We study the constraints using GRBs alone, and further focus on their complementarity to other cosmological probes. In our analyses, We adopt H_0 as a free parameter in the range of $H_0 = 72 \pm 8 \text{ km s}^{-1}\text{Mpc}^{-1}$. In comparison with the results with a strong prior on H_0 (a fixed value of H_0)(Firmani et al. 2006c), the constraints by GRBs alone are much less restrictive. However, the complementarity of GRBs to SNIa are clearly seen, which is mainly contributed by the sub-sample of GRBs with $z>1.5$. This demonstrates the usefulness of high redshift cosmological probes. On the other hand, as BAO highly constraints Ω_M , the contribution of GRBs is degraded by including BAO information in the analyses. The combined analyses of SNIa+GRB+CMB+BAO result constraints on Ω_M and Ω_Λ that are broadly consistent with the concordance Λ CDM model.

We notice the differences between the central values of $(\Omega_M, \Omega_\Lambda)$ from GRBs+SNIa and those from SNIa+BAO. At this stage, we are not able to draw strong conclusions on these because of the large confidence contours. If the differences persist as each of the constraints improves, they might indicate some unknown systematics involved in GRBs, or our knowledge about our universe might not be complete.

The feasibility of GRBs as cosmological probes bridges up the gap between the relatively nearby SNIa and CMB. At present, the quantitative correlations discovered for GRBs are cosmologically model dependent, and therefore there is a notorious circulation problem in applying these correlations to constrain cosmologies. It is thus crucial to find large enough

number of low redshift GRBs (or GRBs in a narrow redshift range) to calibrate the correlations in a model-independent way. On the other hand, to understand the GRB physics more thoroughly may lead to definite correlations between different observables without involving cosmological models. The information on the redshift distribution of GRBs is also of great importance in cosmological studies. Recently, Le and Dermer (2006) found that with the assumption of continued positive evolution of the GRBs rate density to high redshift, the fraction of high-redshift GRBs is estimated to be 8-12% and 2.5-6% at $z \geq 5$ and $z \geq 7$, respectively. With the cumulation of observational data with high qualities, we expect great advances in all this important aspects, and therefore GRBs can provide us much more cosmological information than we have today.

Flat geometry with a relic cosmological term (Λ CDM) seems to be in agreement with almost all the cosmological observations. From the theoretical viewpoint, however, it faces the well-known headache cosmological constant problem (e.g. Weinberg 1989). This and other difficulties motivate different categories of dynamical dark energy models. Current observations provide us only limited knowledge on dark energy, especially on its evolutionary properties. It is therefore of great interests to explore high redshift cosmological probes. GRBs are the only possible candidates for the purpose. In this letter, we concentrate on demonstrating the cosmological roles of GRBs and only present the constraints on Ω_M and Ω_Λ in Λ CDM cosmologies. In our forthcoming paper, we will show the results of global fitting and emphasize the contribution of GRBs to the constraints on the dynamics of dark energy. In short, with limited information from medium and low redshift standard candles such as SNIa so far, high-redshift information from GRBs can help us to shrink the allowed cosmological parameter space, and might further find some interesting behaviors of dark energy at high redshifts. On the other hand, it is theoretically desirable to find out a suitable parametrization of dark energy that could reflect its high-redshift behaviors properly and effectively.

SNIa has been proved playing a central role in elucidating the nature of dark energy. High redshift GRBs as extensions of such standard-candle-like probes are promising and important for cosmological studies. Similar to the anchor for the Hubble diagram provided by low redshift SNIa with $z \sim 0.05$ (Linder 2006), GRBs could perform as a high-redshift hoop helping us to calibrate the middle part of the Hubble diagram more precisely, and thus to get better constraints on the nature of dark energy. Furthermore, high redshift GRBs could directly test exotic dark energy models such as the oscillating dark energy model (Linder 2005) or bump like models (Xia et al. 2004). With CMB from redshift around 1100, 21cm emission and GRBs covering high redshift up to around 80, and SNIa, BAO, weak lensing and Integrated Sachs Wolfe (ISW) effect providing medial and low redshift information, the global picture of the cosmic evolution could be obtained.

M.S. acknowledges valuable discussions with Dai Zigao, Li Hong, Chen Xuelei, Yue Youling and technical supports from Wang Zheng. This research was supported in part by the National Science Foundation of China under grants 10243006 and 10373001, by the Ministry of Science and Technology of China under grant TG1999075401, by the Key Grant Project of Chinese Ministry of Education (305001), and by the National Science Foundation of China under grant 10533010.

REFERENCES

- Aldering, G., Kim, A. G., Kowalski, M., Linder, E. V., Perlmutter, S., 2006, astro-ph/0607030
- Amati, L., Frontera, F., Tavani, M. et al., 2002, A&A, 390, 81
- Astier, P., Guy, J., Regnault, N. et al., 2006, A&A, 447, 31
- Blain, A. W. & Natarajan P., 2000, MNRAS, 312, L35
- Bloom, J. S., Frail, D. A., &Kulkarni, S. R., 2003, ApJ, 594, 674
- Bromm, V. & Loeb, A., 2002, ApJ, 575, 111
- Copeland, E. J., Sami, M., Tsujikawa, S., 2006, hep-th/0603057
- Costa, E., Frontera, F., Heiseet, J. et al., 1997, Nature, 387, 783
- Dai, Z.G., Liang, E.W. & Xu, D., 2004, ApJ, 612, L101
- Daly, R. A. & Djorgovski, S. G., 2004, ApJ, 612, 652
- Eisenstein, D. J., Zehavi, I., Hogget, D. W. et al., 2005, ApJ, 633, 560
- Firmani, C., Avila-Reese, V., Ghisellini, G. & Tutukov A. V., 2004, ApJ, 611, 1033
- Firmani, C., Ghisellini, G., Ghirlanda, G. & Avila-Reese V., 2005, MNRAS, 360, L1
- Firmani, C., Ghisellini, G., Avila-Reese, V. & Ghirlanda G., 2006a, MNRAS, 370, 185
- Firmani, C., Avila-Reese, V., Ghisellini, G. & Ghirlanda, G., 2006b, MNRAS, submitted (astro-ph/0605430)
- Firmani, C., Avila-Reese, V., Ghisellini, G. & Ghirlanda, G., 2006c, MNRAS, submitted (astro-ph/0605267)

- Friedman, A. S. & Bloom, J. S., 2005, ApJ, 627, 1
- Freedman, W. L., Madore, B. F., Gibson, B. K. et al., 2001, ApJ, 553, 47
- Ghirlanda, G., Ghisellini, G. & Lazzati, D., 2004a, ApJ, 616, 331
- Ghirlanda, G., Ghisellini, G., Lazzati, D. & Firmani, C., 2004b, ApJ, 613, L13
- Ghirlanda, G., Ghisellini, G. & Firmani, C., 2006, astro-ph/0610248
- Hooper, D., & Dodelson, S., 2006, astro-ph/0512232
- Lamb, D. Q. & Reichart D. E., 2000, ApJ, 536, 1
- Lamb, D. Q., Ricker, G. R., Lazzati, D. et al., 2005, astro-ph/0507362
- Le, T. & Dermer, C. D., 2006, astro-ph/0610043
- Liang, E. & Zhang B., 2005, ApJ, 633, 611
- Linder, E. V. & Huterer, D. 2003, Phys. Rev. D 67, 081303
- Linder, E. V., 2005, Astropart.Phys. 25, 167
- Linder, E. V., 2006, astro-ph/0609507
- Lloyd-Ronning, N. M., Fryer, C. L. & Ramirez-Ruiz, E., 2002, ApJ, 574, 554
- Lue, A., 2006, Phys. Rept. 423, 1
- Mosquera Cuesta, H. J., Bonilla Quintero, C. A., Habib Dumet, M. et al., 2006, astro-ph/0609262
- Paczynski B., 1998, ApJ, 494, L45
- Peebles, P. J. E. & Ratra, B., 2003, Rev. Mod. Phys. 75, 559
- Pelangeon, A., Atteia, J. L., Lamb, D. Q., Ricker, G. R. et al., 2006, AIPC, 838, 149
- Riess, A. G., Strolger, L-G., Tonry H., et al., 2004, ApJ, 607, 665
- Schaefer, B. E., 2003, ApJ, 583, L67
- Schaefer, B. E., 2006, paper presented at the AAS Meeting January (2006)
- Song, S. Y., Sawicki, I. & Hu, W., 2006, astro-ph/0606286

Spergel, D. N., et al., 2006 astro-ph/0603449;

Tegmark, M., Eisenstein, D., Strauss, M. et al., PRD submitted, astro-ph/0608632

Wang, Y. & Mukherjee, P., 2006, ApJ, in press, astro-ph/0604051

Wang, F. Y. & Dai, Z. G., 2006, MNRAS, 368, 371

Weinberg, S., 1989, Rev. Mod. Phys., 61, 1

Xia, J. Q., Zhao, G. B., Li, H., Feng, B., Zhang, X. M., 2006, Phys. Rev. D 74, 083521

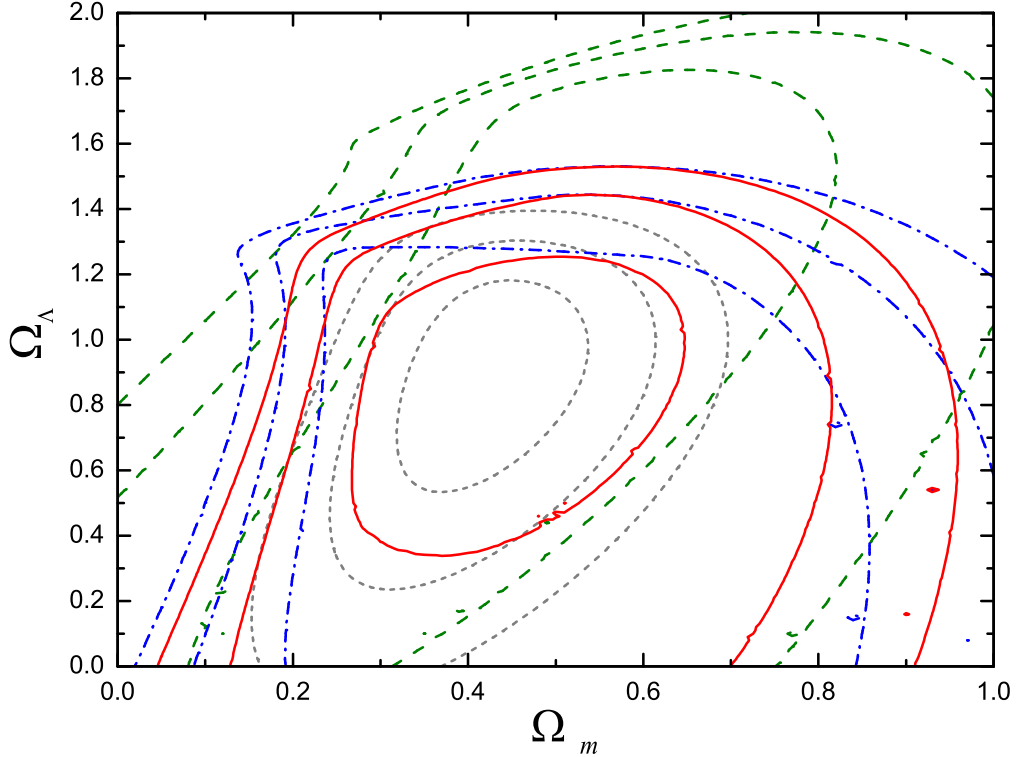


Fig. 1.— 1, 2, and 3 σ confidence level contours on $(\Omega_m, \Omega_\Lambda)$ using the GRB sample. We adopt $H_0 = 72 \pm 8 \text{ km s}^{-1}\text{Mpc}^{-1}$. The dot-dashed lines are the results from the $z > 1.5$ sub-sample with the minimum $\chi^2 = 28.22$ at $\Omega_m = 0.32$ and $\Omega_\Lambda = 0.93$. The dashed lines correspond to the $z < 1.5$ sub-sample with the minimum $\chi^2 = 36.68$ at $\Omega_m = 0.56$ and $\Omega_\Lambda = 1.48$. The solid lines show the constraints resulting from the full GRBs sample with the minimum $\chi^2 = 65.78$ occurring at $\Omega_M=0.43$, and $\Omega_\Lambda=0.91$. The short dashed lines correspond to the full sample constraints with fixed $H_0 = 74 \text{ km s}^{-1}\text{Mpc}^{-1}$. The corresponding minimum χ^2 is $\chi^2 = 65.79$ at $\Omega_m = 0.43$ and $\Omega_\Lambda = 0.91$.

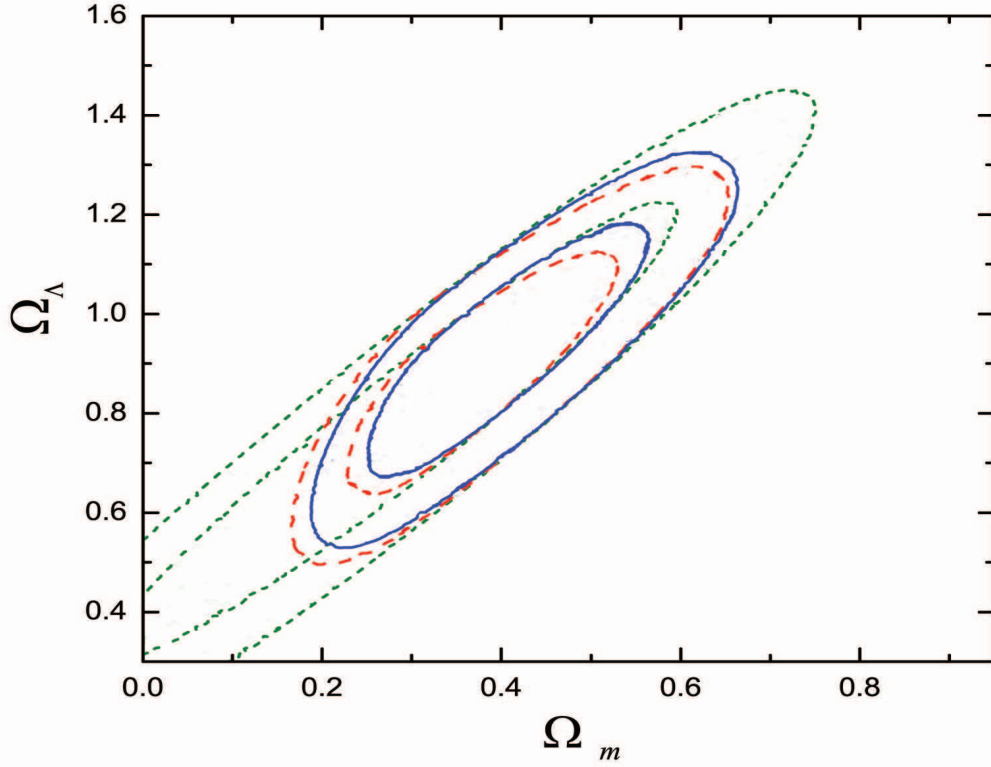


Fig. 2.— 1, 2, and 3 σ confidence level contours for $(\Omega_m, \Omega_\Lambda)$. The short dashed lines correspond to SNLS sample. The dashed lines and the solid lines correspond to constraints combining SNLS with the $z > 1.5$ GRB sub-sample with minimum $\chi^2 = 140.35$ at $\Omega_m = 0.45$ and $\Omega_\Lambda = 1.01$, and with full GRBs sample with minimum $\chi^2 = 181.62$ at $\Omega_m = 0.46$ and $\Omega_\Lambda = 1.02$, respectively.

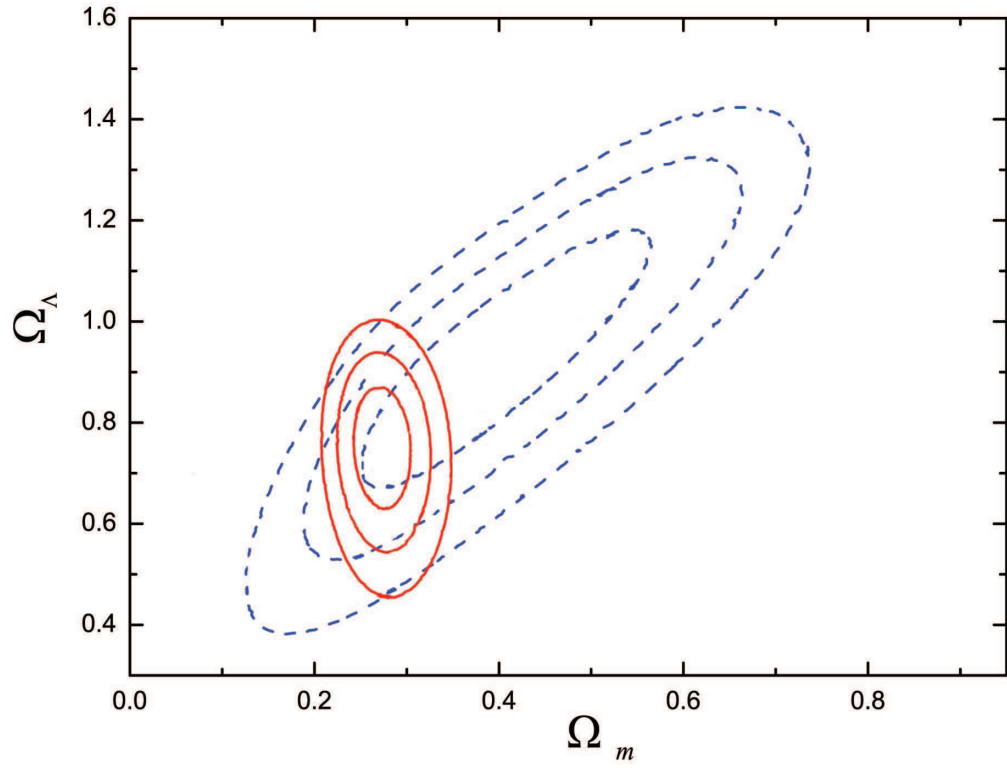


Fig. 3.— 1, 2, and 3 σ confidence level contours for $(\Omega_m, \Omega_\Lambda)$. The solid contours show combined analysis of SNIa + BAO, and the constraints from SNIa + full GRBs sample are shown in dashed lines.

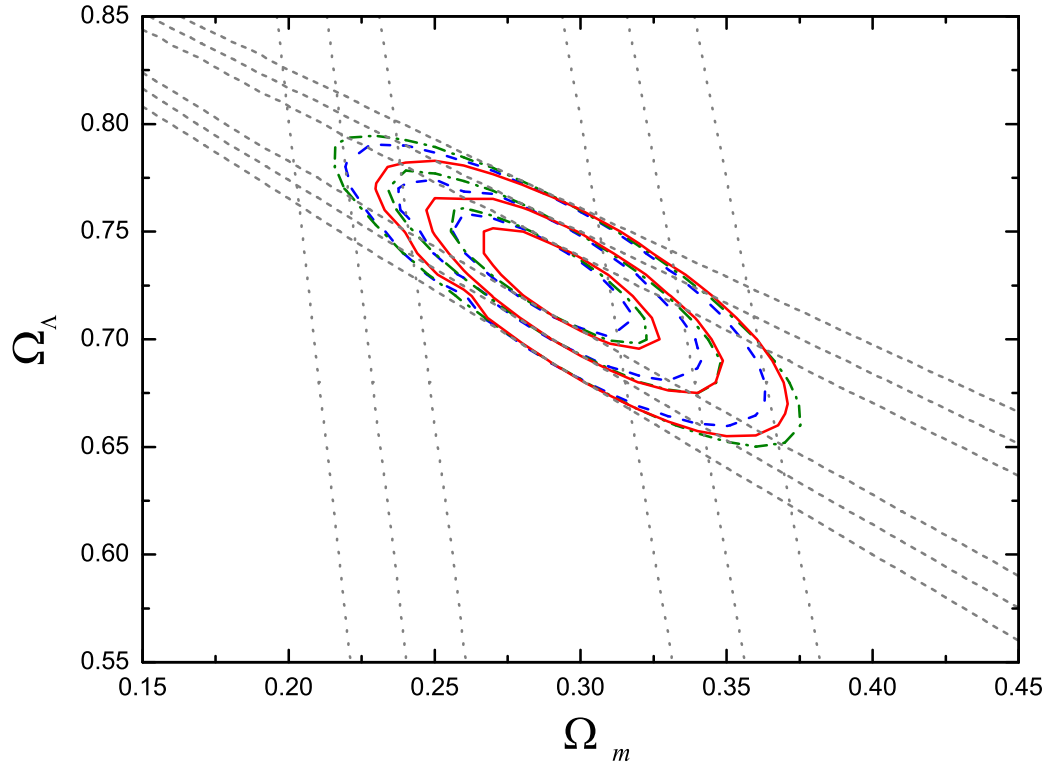


Fig. 4.— 1, 2, and 3 σ confidence level contours for $(\Omega_m, \Omega_\Lambda)$. The dotted lines show constraints from BAO alone, short dashed lines lay out constraints by the CMB shift parameter alone. The combined GRB+CMB+BAO constraints are shown with dot-dashed contours. The dashed contours correspond to CMB+BAO+SNIa and the solid contours correspond to the combined constraints from CMB+BAO+SNIa+GRBs.